

The SINFONI Integral Field Spectroscopy Survey for Galaxy Counterparts to Damped Lyman- α Systems

Céline Péroux¹
 Nicolas Bouché^{2,3}
 Varsha Kulkarni⁴
 Donald York⁵
 Giovanni Vladilo⁶

¹ Laboratoire d'Astrophysique de Marseille, OAMP, Université Aix-Marseille & CNRS, France

² Department of Physics, University of California, Santa Barbara, USA

³ Laboratoire d'Astrophysique de Toulouse-Tarbes, CNRS, Observatoire Midi-Pyrénées, France

⁴ Department of Physics and Astronomy, University of South Carolina, Columbia, USA

⁵ Department of Astronomy and Astrophysics and The Enrico Fermi Institute, University of Chicago, USA

⁶ INAF-Osservatorio Astronomico di Trieste, Italy

A complete picture of galaxy formation can only be obtained by detailed study of the processes by which galaxies convert their gas into stars. One approach is to relate the H I gas and the stars in galaxies. Damped and sub-damped Lyman- α systems (DLAs), which are galaxies probed by the absorption they produce in the spectra of background quasars, are purely selected on H I gas, but identifying the galaxy responsible for the absorber with more traditional methods remains challenging. Integral field spectroscopy provides an efficient way of detecting faint galaxies near bright quasars, further providing immediate redshift confirmation. Here, we report on the detection of DLA and sub-DLA systems identified in H α emission with VLT/SINFONI at near-infrared wavelengths.

Tremendous progress has been made over the last decade in establishing a broad cosmological framework in which galaxies and large-scale structure develop hierarchically over time, as a result of gravitational instabilities in the density field. The next challenge is to understand the physical processes of the formation of galaxies and structures and their interactions with the surrounding

medium. Of particular importance are the processes through which these galaxies accrete gas and subsequently form stars. The accretion of baryonic gas is complex. Recently, several teams have realised that, in halos with mass $< 10^{11.5-12} M_{\odot}$ baryonic accretion may not involve the traditional shock heating process. But the observational evidence for accretion is scarce. A related signature is that the total amount of neutral gas in the Universe, H I, is almost constant over most of the cosmic time (Péroux et al., 2005; Noterdaeme et al., 2009), unlike the history of the star formation rate, which peaks around $z = 1$. This shows the importance of ongoing global gas accretion and the conversion of atomic gas to molecular gas in the star formation process.

One way to tackle these problems is to relate the H I gas and the stars in galaxies. While radio observations now provide detailed constraints on the H I content of large samples of galaxies, they are still limited to redshift $z \sim 0$. Conversely, the study of quasar absorbers, the galaxies probed by the absorption they produce in a background quasar spectrum, is insensitive to the redshift of the object. Indeed, the H I content of the strongest of these quasar absorbers, the so-called damped Lyman- α systems, have been measured in samples of several hundreds of objects from the Sloan Digital Sky Survey (SDSS).

A new observational technique

Nevertheless, studying the stellar content of all these systems turns out to be rather challenging: the galaxies that produce such DLA absorption may be faint, thus requiring deep observations to detect their stellar/interstellar emission; in addition, they have small angular separations from the bright background quasars, which makes it difficult to disentangle the light of the galaxy from that of the quasar. Any broadband identification of a candidate absorber galaxy requires follow-up spectroscopy to confirm that the emission redshift of the object corresponds to the absorption redshift measured in the quasar spectrum. This time-consuming step is sometimes missing, thus complicating the interpretation of the

observations made so far. As a result of these issues, only 15 spectroscopically confirmed identifications of DLA/sub-DLA galaxies with measured $N_{\text{H I}}$ are known at cosmological redshift $z < 1$ and five at $z > 1$.

Imaging spectroscopy at near-infrared (NIR) wavelengths with adaptive optics can be used to solve the above-mentioned problems efficiently. The advantages afforded by this technique are manifold:

- 1) The contribution from the quasar is deconvolved from the absorber in the spectral dimension, thus allowing virtually zero impact parameters to be reached if the flux of the galaxy is greater than the quasar continuum flux.
- 2) The data provide a spectrum of the absorbing galaxy for immediate redshift confirmation.
- 3) The detection of nebular emission lines such as H α , a robust estimator of star formation rate, redshifted to the NIR at $z > 0.6$, can give clues to the stellar content of the galaxy and metallicity of the warm gas producing the nebular lines.
- 4) The spatially resolved kinematic data provide information on the dynamical state of the system.

The powerful combination of an 8-metre class Very Large Telescope (VLT) and the SINFONI instrument has been successfully pioneered by Bouché et al. (2007). These authors have detected 67% (14 out of 21) of the systems in a sample of Mg II absorbers at $z \sim 1$. The H α detections are used to derive star formation rates of the order 1–20 M_{\odot}/yr . Their observations are sensitive to fluxes $F(\text{H}\alpha) > 1.2 \times 10^{17} \text{ erg s}^{-1} \text{ cm}^{-2}$, corresponding to star formation rates of $\sim 0.5 M_{\odot}/\text{yr}$. Interestingly, lower detection rates are found at higher redshifts around $z \sim 2$ (Bouché et al., 2011). Here, we report the first results of our H I-selected survey aimed at detecting the host galaxies via their H α signature. In the present work, we report the detections of two DLA/sub-DLAs at $z \sim 1$ for which $N_{\text{H I}}$, and hence absorption metallicities, are known from high resolution spectroscopy out of five quasar fields with intervening absorbers (one with two sub-DLAs) searched.

New detections

The observations presented here were carried out with the NIR integral field spectrometer SINFONI on Unit Telescope 4 of the VLT during three separate observing runs (ESO 79.A-0673, 80.A-0330 and 80.A-0742). In Péroux et al. (2011a), we have reported detections of a DLA with $\log N_{\text{H I}} = 20.36 \pm 0.11$ at $z_{\text{abs}} = 1.009$ towards Q0302-223 (see Figure 1) and a sub-DLA with $\log N_{\text{H I}} = 19.48 \pm 0.05 - 0.06$ at $z_{\text{abs}} = 0.887$ towards Q1009-0026 (see Figure 2). We detect galaxies associated with the quasar absorbers at impact parameters of 25 and 39 kpc away from the quasar sight-lines, respectively.

For the field of Q0302-223 where the quasar is bright enough, we have used the quasar itself as a natural guide star for adaptive optics in order to improve the spatial resolution. Using the $\text{H}\alpha$ luminosity we derived the star formation rate assuming the Kennicutt (1998) flux conversion, corrected to a Chabrier (2003) initial mass function. These findings are summarised in Table 1. We find low star formation rates; these values of star formation rates are among the lowest that have ever been possible to detect in quasar absorber searches with ground-based observations at $z \sim 1$.

Comparison with other detected absorbers

We have made a careful reappraisal of published reports of detections of galaxies responsible for DLA and sub-DLAs. Figure 3 shows the relation between several of the properties. The triangles represent limits and the measurements reported in the present article are circled in red. From this figure, it appears that the detected objects in the sample are mostly low luminosity and low star formation rate galaxies, yet the galaxies have a wide range of luminosities. We also note

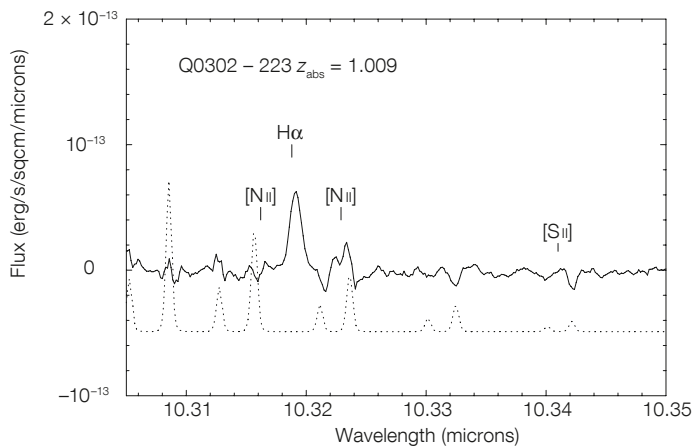


Figure 1. The integrated spectrum of the corresponding DLA galaxy with the expected $\text{H}\alpha$, $[\text{N II}]\lambda 6585$ and $[\text{S II}]\lambda 6718$ doublet positions indicated at $z_{\text{em}} = 1.00946$. The dotted spectrum at the bottom of the panel is the sky spectrum indicating the position of the OH sky lines. In this case, $[\text{S II}]$ is not detected and an upper limit is derived due to contamination by an OH sky line.

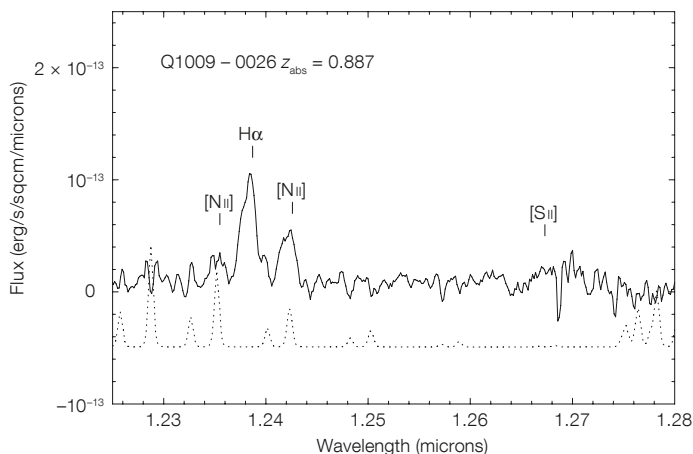


Figure 2. The integrated spectrum of the galaxy with the expected $\text{H}\alpha$, $[\text{N II}]$ and $[\text{S II}]$ line positions indicated at $z_{\text{em}} = 0.88637$. $[\text{N II}]\lambda 6585$ is affected by an OH sky line but this is much narrower than the line we detect and $[\text{S II}]$ is not detected.

that small impact parameters ($b < 30$ kpc) dominate and that very few galaxies are identified beyond 40 kpc, which matches the search radius in our SINFONI study well. Removing the outlier with $\log N_{\text{H I}} = 21.71$ and $b = 44$ kpc, we find a weak negative correlation, where higher $N_{\text{H I}}$ absorbers have smaller impact parameters. Also it is interesting to note that the highest $N_{\text{H I}}$ column density seems to have higher L/L_* ratio. The Spearman rank correlation coefficient indicates that the two are weakly correlated. Although the scatter is large, the reported absorption metallicities do not vary much

with impact parameter. It is also clear that abundances reported in absorption are not well-correlated with emission abundances.

Metallicity

Unlike most of the objects in Figure 3, and other objects reported at these redshifts, the galaxies that we have detected in this study have well-known absorption metallicities from high resolution UV spectroscopy. Using the N_2 parameter (Pettini & Pagel, 2004) based

Table 1. Summary of the properties of two Ly α absorber galaxies detected with SINFONI.

Quasar	z_{abs}	$\log N(\text{H I})$ (atoms/cm ²)	$[\text{Zn}/\text{H}]$	Impact parameter (kpc)	$F(\text{H}\alpha)$ (erg/s/cm ²)	Lum($\text{H}\alpha$) (erg/s)	SFR M_{\odot}/yr
Q0302-223	1.009	$20.36^{+0.11}_{-0.11}$	-0.51 ± 0.12	25	$7.7 \pm 2.7 \times 10^{-17}$	$4.1 \pm 1.4 \times 10^{41}$	1.8 ± 0.6
Q1009-0026	0.887	$19.48^{+0.05}_{-0.06}$	-0.25 ± 0.06	39	$17.1 \pm 6.0 \times 10^{-17}$	$6.6 \pm 2.3 \times 10^{41}$	2.9 ± 1.0

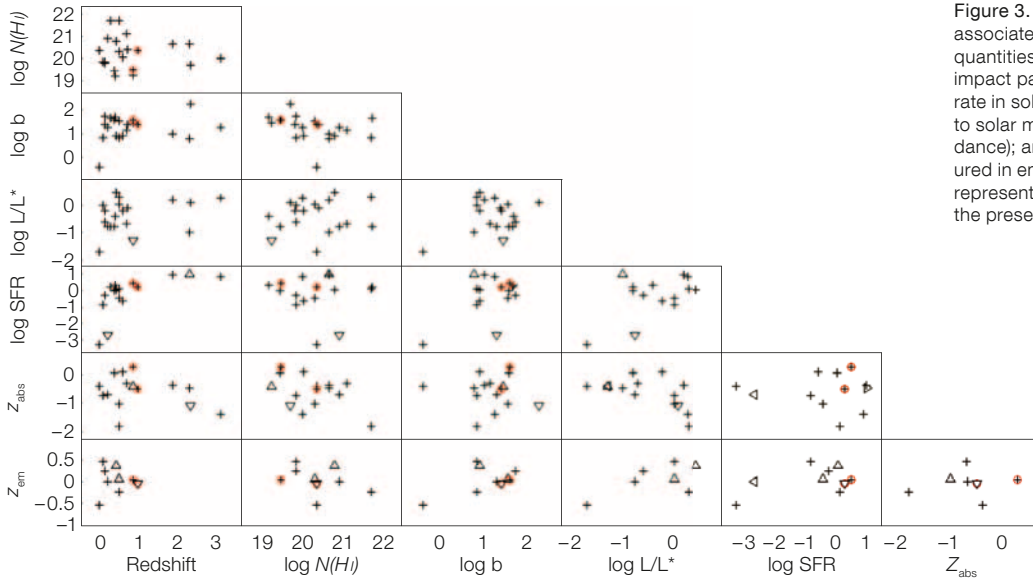
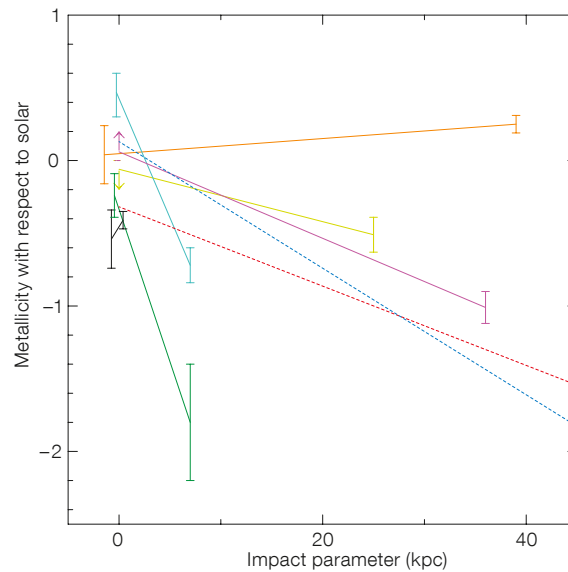


Figure 3. Correlation plots for the detected galaxies associated with DLAs and sub-DLAs. The following quantities are plotted: redshift; $N_{\text{H I}}$ column density; impact parameter in kpc; luminosity; star formation rate in solar masses per year; metallicity with respect to solar measured in absorption, Z_{abs} (H I abundance); and metallicity with respect to solar measured in emission, Z_{em} (H II abundance). The triangles represent limits and the measurements reported in the present article are circled in red.

Figure 4. Metallicity with respect to solar measured in emission at impact parameter $b = 0$ and in absorption at given impact parameters in kpc. The two metallicities arising from the same galaxy are linked by coloured lines. The arrows indicate upper and lower limits on the measure of the emission metallicities. The errors on the emission metallicities are artificially offset from $b = 0$ for clarity. The two dotted lines are the H II region oxygen abundance gradients measured in M101 (slope = -0.043 dex/kpc, in blue) and M33 (slope = -0.027 dex/kpc, in red) for comparison.



on $[\text{N II}]\lambda 6585/\text{H}\alpha$ ratio, we can derive an estimate of the emission metallicity. For the DLA towards Q0302-223, we find about solar abundance, compared to the one-third solar metallicity reported in absorption ($[\text{Zn}/\text{H}] = -0.51 \pm 0.12$). For the sub-DLA towards Q1009-0026, we find slightly above solar metallicity, compared with a super-solar absorption metallicity ($[\text{Zn}/\text{H}] = +0.25 \pm 0.06$).

In order to investigate the role that gradients might play in the difference between the emission and absorption

abundances, we have plotted the metallicity with respect to solar as a function of the impact parameter in Figure 4.

Clearly, in most of the six cases plotted here, the metallicity measured at a larger radius is lower than the one measured in the centre, sometimes with a slope steeper than that observed in local galaxies. In the case of Q1009-0026, however, the metallicity at the centre of the galaxy (seen in emission) is lower than the metallicity at 39 kpc radius (seen in absorption). This surprising result might just be the result of an uncertain

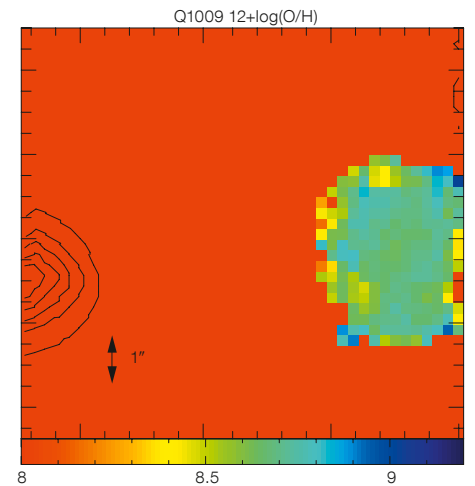


Figure 5. This figure presents the metallicity in units of $12+\log(\text{O}/\text{H})$ derived from the N_2 parameter, i.e. the ratio of $[\text{N II}]\lambda 6585/\text{H}\alpha$, in Q1009-0026. The metallicity appears to be rather uniform on this scale, as expected from the magnitude of the gradients observed in such objects (see Figure 4).

measurement as reflected by the large error bar (see Figure 4). It might also be partly explained by the use of the metallicity indicator. Indeed, Pettini & Pagel (2004) have demonstrated that the N_2 -parameter/metallicity relation has a rather large scatter at high metallicities, where these data lie. In addition, it should be emphasised that these measurements are not tracing the same gas phase (neutral versus ionised gas). However, it is interesting to note that at $z \sim 3$,

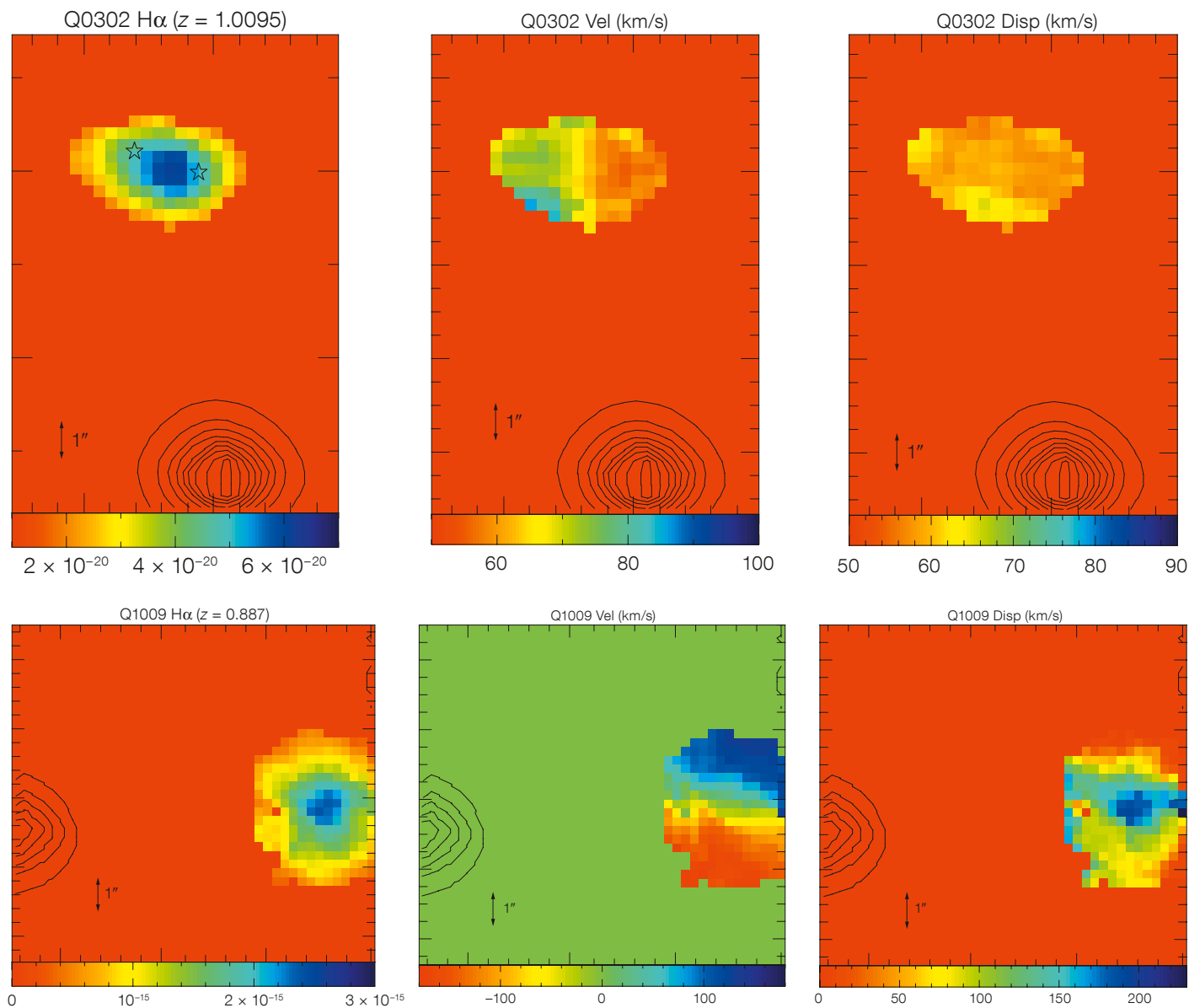


Figure 6. H α flux map, H α velocity field and H α velocity dispersion maps of the quasar absorbers Q0302-223 (upper) and Q1009-0026 (lower). The colour scale indicates the flux in $\text{erg s}^{-1} \text{cm}^{-2}$ in the H α flux map on the left and the velocities and velocity dispersions in km/s for the middle and right set of panels. North is up and east is to the left. The thin black contours indicate the position of the quasar.

there have been detections of inverted gradients, interpreted as a signature of accretion, but on a much smaller distance scale (Cresci et al., 2010).

Finally, we use the spatial information made available to us from the 3D spec-

troscopy to compute a metallicity map of Q1009-0026. Figure 5 presents the metallicity in units of $12+\log(\text{O}/\text{H})$ derived from the N_2 parameter (Pettini & Pagel, 2004), i.e. the ratio of $[\text{N II}]\lambda 6585.27/\text{H}\alpha$. The metallicity gradient appears to be rather uniform on that scale, as expected from the magnitude of the gradients observed in such objects (see Figure 4).

Kinematics

In addition to the identification and redshift confirmation of the galaxy responsible for

the quasar absorbers, the SINFONI data allow for a study of the dynamical properties of the galaxies. We extracted maps of the velocity-integrated line fluxes, relative velocities, and velocity dispersion from the reduced data cubes (Figure 6). Using these maps, critical information on the dynamical state and properties of the galaxies associated with quasar absorbers can be derived.

The galaxy associated with the $z_{\text{abs}} = 1.009$ DLA towards Q0302-223 shows little sign of rotation or significant amounts of dispersion. It has an axis

Quasar	$\sin i$	v/σ	$r_{1/2}$ (")	Σ_{SFR} ($M_{\odot}/\text{yr}/\text{kpc}^2$)	M_{dyn} (M_{\odot})	Σ_{gas} (M_{\odot}/pc^2)	M_{gas} (M_{\odot})	M_{halo} (M_{\odot})	M_{*} (M_{\odot})
Q0302–223 ^a	0.88	0.19	0.7	0.13	$10^{10.3}$	$10^{1.9}$	$10^{9.1}$	–	$10^{9.5}$
Q1009–0026	0.60	1.45	0.5	0.31	$10^{10.9}$	$10^{2.2}$	$10^{9.2}$	$10^{12.6}$	–

ratio of $b/a = 0.47$ corresponding to an inclination of $\sin i = 0.88$. The maximum velocity is $V_{max} = 11$ km/s. The ratio v/σ in this object is 0.19 (see Table 2), much smaller than seen in local disc galaxies ($v/\sigma = 10\text{--}20$ km/s), and at high redshift. This might indicate that this object is pressure-supported, and early-type morphologies come to mind. However, the morphology of this object indicates that this galaxy might be a late-type object. The SINFONI data show that it is highly elongated. This is supported by the archival HST/WFPC2 images covering this field (Le Brun et al., 1997). In these data, two separate components can be seen, but their redshifts cannot be estimated (see the two stars in Figure 6 [upper flux map] which indicate the positions of the components). The two individual components are not resolved in the SINFONI observations and might explain the elongated shape; alternatively only one component is seen but the detection of H α emission at the position of the absorber provides secure identification. One interpretation is that we might be seeing a dispersion due to a small difference in redshift of two interacting galaxies. However, the H α light profile appears to be exponential with a scale length of 0.6 arcseconds. Thus, an alternative explanation is that this galaxy is dispersion-dominated, although it already has a disc-like morphology. This is indicative of a young attenuated object, with effective radius (containing half of the light) of $R_e = 0.5$ arcseconds, or 4 kpc, whose kinematics show that sustained rotation has not yet occurred. In other words, this object will have to contract further.

By contrast, the absorber toward Q1009-0026 has a morphology and kinematics consistent with that of a disc, with a normal dispersion profile ($v/\sigma = 1.45$) peaking at the centre $\sigma_{peak} = 190$ km/s and flattening in the outer parts to $\sigma_{disc} = 60\text{--}70$ km/s (see Table 2). This object is more face-on with an estimated inclination of $\sin i = 0.60$ derived from

an axes ratio $b/a = 0.80$. It shows clear signatures of rotation with systematic velocity gradients. Its v/σ is not typical of local disc galaxies, which have $v/\sigma = 10\text{--}20$, but the systematic gradient still favours a spiral galaxy.

We also use the kinematic maps to estimate the sizes of the systems. These, in turn, are used to compute the area of the objects assuming that the inclined discs appear as ellipses. Using these estimates of the sizes of the detected galaxies, we compute their star formation rate surface densities (see Table 2).

Mass estimates

The observations provide direct observational estimates of dynamical masses for galaxies selected on neutral gas H I content (see Table 2). In order to estimate the mass of gas in these objects, we start from the observed H α surface brightness and compute gas surface brightness using an inverse Schmidt–Kennicutt relation. The results indicate a low gas fraction in the objects. In addition, both objects show clear exponential light profiles indicative of discs. Thanks to our kinematical data based on the H α emission line widths, we are able to estimate the mass of the halo in which the system towards Q1009-0026 resides. The halo mass we derive is comparable with the one from the Milky Way. In the case of the DLA towards Q0302-223, we use the broadband magnitudes from HST/WFPC2 (Le Brun et al., 1997) and ground-based NIR observations (Chen & Lanzetta, 2003) which cover the Balmer break of the object to constrain the age of the stellar population in the galaxy with a spectral energy distribution fitted to the integrated light of the galaxies. The spectroscopic redshift and star formation rate derived from our SINFONI spectra are used as an input to the code, thus allowing the stellar mass of the object to be constrained with relatively high confidence, and, in turn, allows us to put

Table 2. Kinematic properties and mass estimates of the two N_{HI} absorbers detected.

Note: The inclination is the main source of uncertainties and is estimated to be around 30 %.

^a The higher resolution HST/WFPC2 data from Le Brun et al. (1997) clearly shows that the object is subdivided into two sub-components, consistent with the elongated shape seen in the SINFONI data presented here. In this table, however, the object is treated as single.

constraints on the baryonic mass fraction in this galaxy. We derive a gas fraction of one third. Such gas fractions are in the low range of the typical values derived in $z \sim 2\text{--}3$ galaxies by others. When comparing these various mass estimates, we see that these systems have little room for molecular gas, which is consistent with the low star formation rates derived.

Future prospects

The observational set-up of SINFONI has demonstrated the power of integral field spectroscopy for deriving a number of emission properties for quasar absorbers, a type of high-redshift galaxy that has been difficult to identify in the past. These new tools are now available to study these objects systematically and work is continuing to expand the survey with three new additional detections recently reported (Péroux et al., 2011c). This type of study illustrates that detailed studies of quasar absorbers can offer entirely new insights into our knowledge of the interaction between stars and the interstellar gas in galaxies.

References

- Bouché, N. et al. 2007, ApJ, 669, L5
- Bouché, N. et al. 2011, MNRAS, submitted
- Cresci, G. et al. 2010, Nature, 467, 811
- Le Brun, V. et al. 1997, A&A, 321, 733
- Noterdaeme, P. et al. 2009, A&A, 505, 1087
- Pettini, M. & Pagel, B. E. J. 2004, MNRAS, 348L, 59
- Péroux, C. et al. 2005, MNRAS, 363, 479
- Péroux, C. et al. 2011a, MNRAS, 410, 2237
- Péroux, C. et al. 2011b, MNRAS, 410, 2251
- Péroux, C. et al. 2011c, MNRAS, submitted